The effects of climate change on Chinese Medicinal Yam over North China under the high-resolution PRECIS projection

Dongli Fan[1], Zhiyu Jiang[2], Zhan Tian[3], Guangtao Dong[4], and Laixiang Sun[5]

[1]Shanghai Institute of Technology
[2]School of Atmospheric Sciences, Nanjing University
[3]School of Environmental Science and Engineering, Southern University of Science and Technology
[4]Shanghai Climate Center
[5]University of Maryland, College Park

November 24, 2022

Abstract

The arid and semi-arid regions are highly vulnerable to climate change and variability. Agricultural production in these regions is particularly vulnerable because of its heavy dependence on on climate conditions. Therefore, it is important to improve the projections of future agro-climatic conditions. This study investigates the projections of agroclimatology change during 2031–2050 under the Representative Concentration Pathway (RCP) 8.5 emission scenario in the semi-arid North China. It is simulated by the agro-ecological zone (AEZ) model with climate data provided by the regional climate model (RCM) of Providing regional Climates for Impacts Studies (PRECIS). The Chinese Medicinal Yam (CMY), which is genuinely produced over semi-arid regions, is taken as an example to study the change of its yield and producing area under future climate change. The results show that the high-resolution RCM simulation corresponds better with the observations than the general circulation model (GCM) in precipitation and temperature. In North China, the CMY genuine production area, the precipitation will increase by about 10% and the temperature will increase by about 2°C under the RCP8.5 scenario. After the evaluation and projection of climate models, the potential yield of CMY and the suitable planting regions are simulated by using the AEZ model. The CMY production areas will expand northward in the future, due to the climate warming in the north. The traditional yam production area still maintains the suitability of CMY production. The production of CMY will augment because of the increased production area.

The effects of climate change on Chinese Medicinal Yam over North China under the high-resolution PRECIS projection

Dongli Fan[1], Zhiyu Jiang[2], Zhan Tian[3,*], Guangtao Dong[4,5], Laixiang Sun[6,7,*]

[1] Shanghai Institute of Technology, Shanghai, 201400, China

[2] School of Atmospheric Sciences, Nanjing University, Nanjing, 210023, China;

[3] School of Environmental Science and Engineering, Southern University of Science and Technology, Shenzhen, 518055, China

[4] Shanghai Climate Center, Shanghai, 200030, China

[5] Key Laboratory of Cities' Mitigation and Adaptation to Climate Change in Shanghai, China Meteorological Administration, Shanghai, 200030, China

[6] Department of Geographical Sciences, University of Maryland, College Park, MD 20742, USA

[7] School of Finance and Management, SOAS University of London, London WC1H 0XG, UK

Corresponding author: Zhan Tian (tianz@sustech.edu.cn)

Laixiang Sun (LS28@soas.ac.uk; LSun123@umd.edu)

Key Points:

- Improving the projections of future agro-climatic conditions in the semi-arid North China.
- The high-resolution PRECIS projection correspond better with the observations.
- The CMY production areas will expand northward in the future, due to the climate warming.

The effects of climate change on Chinese Medicinal Yam over North China under the high-resolution PRECIS projection

Abstract

The arid and semi-arid regions are highly vulnerable to climate change and variability. Agricultural production in these regions is particularly vulnerable because of its heavy dependence on on climate conditions. Therefore, it is important to improve the projections of future agro-climatic conditions. This study investigates the projections of agroclimatology change during 2031–2050 under the Representative Concentration Pathway (RCP) 8.5 emission scenario in the semi-arid North China. It is simulated by the agro-ecological zone (AEZ) model with climate data provided by the regional climate model (RCM) of Providing regional Climates for Impacts Studies (PRECIS). The Chinese Medicinal Yam (CMY), which is genuinely produced over semi-arid regions, is taken as an example to study the change of its yield and producing area under future climate change. The results show that the high-resolution RCM simulation corresponds better with the observations than the general circulation model (GCM) in precipitation and temperature. In North China, the CMY genuine production area, the precipitation will increase by about 10% and the temperature will increase by about 2°C under the RCP8.5 scenario. After the evaluation and projection of climate models, the potential yield of CMY and the suitable planting regions are simulated by using the AEZ model. The CMY production areas will expand northward in the future, due to the climate warming in the north. The traditional yam production area still maintains the suitability of CMY production. The production of CMY will augment because of the increased production area.

1 Introduction

The Intergovernmental Panel on Climate Change (IPCC) published a special report indicating that the global average temperatures have increased by about 1°C since the pre-industrial era, and the anthropogenic warming contributes around 0.2°C increase to global average temperatures every decade (IPCC, 2018). Also, the global average warming reaching about 1.5°C between 2030 and 2052 is projected in the report at the present anthropogenic greenhouse gas (GHG) emissions. Climate is one of the most critical limiting factors for agricultural production (Moonen et al., 2002). It is expected that the climate change will significantly influence the food production no matter on regional scale or global scale. The change of temperature regimes and precipitation and the like agroclimatic conditions will vary the crop suitability and soil moisture conditions (Fischer et al., 2005). Relatively small changes in the mean values of rainfall and temperature can significantly affect the frequency of extreme levels of available warmth and moisture (Parry, 2019). The annual mean temperature increases only 1 or 2 ºC could result in significant growth of scorching days which has devastating impact on crops and livestock. Likewise, the average soil moisture decrease resulting from higher evapotranspiration rates could substantially raise water shortage days for crops.

Global climate models (GCMs) are constructive for predicting future climate changes. Many studies have provided in-depth explanations of future climate changes and their impacts based on GCMs (Xu et al., 2019; Chen et al., 2019; Sun et al., 2015). The accuracy of current GCMs has become higher and higher, but there are still limitations in representing small-scale processes that affect the local climate (Han et al., 2019). The dynamic downscaling method uses regional climate models (RCMs) to generate more regional or local climate information (Giorgi et al., 2009), as a balance of computational resource and resolution demand. Therefore it has become one of the commonly used methods for obtaining high-resolution climate simulation and prediction. Down-scaled regional climate information is vital for quantitative impact assessment and risk analysis (such as water resources and water-related disasters). In China, many climate simulations and predictions based on RCMs have been carried out (Park et al., 2019; Duan et al., 2019; Niu et al., 2018; Jiang et al., 2020; Dong et al., 2020). The studies found that, compared with GCMs, RCMs have superior performance in climate simulations (Gu et al., 2018; Hui et al., 2018), can reduce precipitation overestimation in some areas (Zhang et al., 2017), and can provide a more reliable extreme value index (Bucchignani et al., 2017; Kong et al., 2019). However, the RCMs used in previous studies are still too rough to represent some surface details. The horizontal grid spacing is usually 30–60 km, which gradually cannot meet the operational requirements for accuracy. A common belief is that higher resolution brings more realistic simulation in a certain range, along with the precipitation of physical process. Climate predictions with high resolution are still too few to give credible results. Therefore, higher-resolution RCMs are needed to obtain more reliable climate simulations and projections.

The future climate changes rapidly in arid and semi-arid regions (Dong et al., 2020). Further studies are needed over there about the responses of the crop growth or yield (Bouras et al., 2019). According to Li et al. (2015), Chinese semi-arid regions have expanded during the last 60 years, and the northeastern China has suffered from droughts, while the northwestern China has experienced less-severe droughts. Arid and semi-arid areas may be susceptible to longer duration dry-spells and more frequent drought (Waldman et al., 2019), facing the developing risk from climate change (Xia et al., 2017). Thus, it is essential to develop appropriate strategies to cope with significant semi-arid climate change and maintain sustainable development in these regions (Huang et al., 2019). Due to the importance of semi-arid regions, many studies have been carried out worldwide (Du et al., 2019; Yang et al., 2019; Fernández et al., 2019). In China, by using multi GCMs Wang et al. (2019) discovered the great uncertainty of precipitation change in the inland arid region of Northwest China. Using an RCM with a horizontal grid spacing of 0.5°, Xu et al.

(2017) found significant increase in the surface air temperature at 2 m height by 1–1.5°C especially in the warm days from 1980 to 2014.

Though climate assessments have been made in the semi-arid regions of China, there is still little researches about the influence of climate change to the agricultural production based on a high-resolution RCM. Many researches focused on the statistical analysis of historical change (Kukal et al., 2018), or lacked a higher resolution prediction of future agroclimatology changes (Mo et al., 2017), or did not combine with the crop yield (Shkolnik et al., 2019). Tian et al. (2014) used high-resolution climate scenarios from RCMs as the input to the agro-ecological zone (AEZ) model for China, and computed a comprehensive set of agroclimatic indicators. Nevertheless, they did not have an exact prediction of any crop. The combination of the regional climate model and crop model has been delivered in many parts of the world (Kourat et al., 2020; Singh et al., 2018). In China, Zou et al. (2019) evaluated the performance of a coupled climate-crop model based on RegCM4 (Regional Climate Modeling system version 4) at 0.5° grid spacing, finding a great ability to simulate the phenological change and spatial variation of crops, but they did not give a projection of the future crop yield. The future agroclimatic conditions based on high-resolution RCM projections in arid and semi-arid regions of China is still a question worth studying.

Climate factors could largely affect the yield and quality of Chinese Medicinal Yam (CMY) (Hu et al., 2018). The Chinese herbal medicine has obvious geographical distribution characteristics. With genuine CMY growing in the semi-arid and semi-wet regions of North China, it is essential to evaluate the future ecological suitability of CMY planting area. Geographic Information System technology is used by Hu et al. (2018) to evaluate the ecological suitability of planting area by the similarity classification, instead of climate models. Fan et al. (2019) simulated the yield variations of CMY with the AEZ model driven by several GCMs. They found the agroecological suitability of CMY in the northern Shaanxi, the eastern Shandong, the eastern Hebei and some parts of northeastern China will be improved because of the improved hygrothermal conditions. However, there is a shortage of CMY yield simulations based on high-resolution RCM.

This study combines the crop model (AEZ) and the high-resolution RCM (PRECIS, 0.25° grid spacing), and uses the updated CMY parameters from Fan et al. (2019) to further understand the agroclimatology and agricultural production in the semi-arid regions of China. The remainder of this paper is organized as follows. Section 2 provides details of the experiment design and reference datasets. Section 3 presents the evaluation of RCM simulations and the projection of CMY production over China. The results are summarized in Section 4.

2 Data and Methods

2.1 Observation

CN05.1 dataset is interpolated from over 2400 observing station in China, with the resolution of $0.25° \times 0.25°$ (longitude × latitude). The climatology is first interpolated by thin plate smoothing splines and then a gridded daily anomaly derived from angular distance weighting method is added to climatology to obtain the final dataset (Wu d Gao, 2013). The dataset includes daily temperature and precipitation from 1961-2005. It has been used for verification in many studies. CRUTS32 (Climatic Research Unit gridded Time Series v3.2) is a widely used climate dataset with the resolution of $0.5° \times 0.5°$ over all land domains of the world except Antarctica. It is interpolated by the monthly weather station observations across the world, containing climate variables such as mean temperature, diurnal temperature range and precipitation (Harris et al., 2014).

2.2 Climate models

HadGEM2-ES (Hadley Center Global Environment Model, version 2) is a coupled AOGCM with atmospheric resolution of N96 ($1.875^{\circ} \times 1.25^{\circ}$) with 38 vertical levels and an ocean resolution of 1° (increasing to $1/3^{\circ}$ at the equator) and 40 vertical levels. It in-corporates elements of dynamic vegetation, marine biological processes, sea ice, tropospheric chemistry and the carbon cycle over land and ocean (Bellouin et al., 2011).

PRECIS is a regional climate simulation system based on GCM-HadCM3 developed by the Hadley Centre for Climate Prediction and Research, Met Office, UK. Its horizontal resolution is 50 km or 25 km. With HadRM3P (RCM) as its core component, PRECIS can operate in any limited region of the world. The model includes the atmospheric dynamic processes, sulfide cycle and related atmospheric and land surface physical processes. The model's physical processes include cloud and precipitation, convection, radiation, boundary layer, land surface exchange and gravity wave resistance (Wu et al., 2020). The model convection scheme adopts the mass flux penetrating cumulus scheme, and considers the influence of vertical convective momentum. The land surface scheme adopts the updated version of the Met Office surface exchange scheme (Moses), and uses the improved subgrid technology to splice vegetation information and soil type information. The dynamic part of the model includes dynamic processing of the evolution of meteorological variables such as wind and temperature, and the continuous improvement of physical process parameterization of humidity and pressure (Guo et al., 2019). It is based on the atmosphere part of HadGEM2-ES to provide boundary conditions and initial fields, and to run again based on its relatively low-resolution grid.

PRECIS is driven by high-resolution side boundary conditions generated by HadRM3P, and uses the quasi-hydrostatic balance equation to deal with the atmospheric part. It has 19 vertical levels, with the top being 0.5 hPa. The bottom four levels in the vertical direction adopt the terrain-following σ coordinate system, the top three levels adopt the P coordinate system, and the middle levels adopt the hybrid coordinate system. In the horizontal direction, the Arakawa B grid is used for calculation, and the horizontal diffusion term is used to control the nonlinear instability. The horizontal resolution of the bottom level (surface) in the rotating coordinate system is 0.22° (longitude) × 0.22° (latitude), the horizontal interval is about 25km in the middle latitude region, and the integration step length is 5 min. The historical simulation period is 1986-2005 and the future period is 2031-2050.

2.3 AEZ model

The AEZ model used in this study is jointly developed by the Food and Agriculture Organization of the United Nations (UN-FAO) and the International Institute for Ap-plied Systems Analysis (IIASA), and it is mainly used for crop-suitability assessment and productivity-potential calculation. The agricultural ecological region model is widely used in various fields. It takes radiation, light, precipitation, temperature, soil and other ecological factors into consideration, and constructs the feedback mechanism of climate soil-plant interaction. Due to the relatively rigorous calculation process of production potential, the model has been widely used in agricultural evaluation and has achieved good results (Fischer et al., 2000; Fischer et al., 2002). The AEZ model gradually modifies the maximum bio-logical yield of crops by limiting parameters (such as cumulative temperature, humidity, soil suitability and management methods), and could simulate the maximum yield. The AEZ model is supported by crop growth algorithm and environment matching program, and it is very suitable for large-scale crop productivity assessment (Fischer et al., 2005; Tian et al., 2012).

The model calculates the production potential under different conditions step by step, considering the input level and management measures in the production process. The final agricultural production potential is obtained under the chosen condition of heat, light and the like. When the temperature, soil moisture, soil pH and other soil conditions are in the most appropriate state, the model only considers the impact of light on the production potential that is called the photosynthetic potential. Similarly, solar and temperature potential productivity is the crop yield under the influence of light and temperature at the same time while other conditions at the most appropriate state. It is a temperature correction over the photosynthetic productive potential. Land production potential takes integrating climate productivity and the soil availability coefficient into consideration based on prior potential. The relative importance of each influencing factor is assessed by the key information of soil pH value, texture, soil nutrient (N, P, K) content and slope, which results in the weight coefficients of each soil availability factor. Then the soil availability coefficient is obtained by integrating each influencing factor. The above calculation only considers the land productivity, that is, the productive potential excluding the influence of non-natural factors. The agricultural production potential is defined as the comprehensive evaluation of crop production potential considering the impact of different economic input and management measures. In the AEZ model, economic input can choose high, middle or low conditions. This paper chooses the high input level. In this paper, the crop production potential under a high input level is calculated.

In the past 50 years, the original parameters in the AEZ model are not representative in the middle and high latitudes due to climate warming. Moreover, the parameters for yam in the model are set for dioscoreaceae, which is not suitable for the typically Chinese medical yam. At present, the parameters of CMY have been updated in Table 1 by Fan et al. (Fan et al., 2019). Focus on medicine property of CMY, Fan et al. chose the climate factors in the genuine CMY producing areas to update CMY-dedicated physiological and ecological parameters in the AEZ model. In this study, new CMY varieties are introduced into the AEZ model, and then the AEZ model is applied to evaluate the CMY suitability under potential climate conditions in China. Some advantages of AEZ model are the high calculating speed and the expansibility to incorporate climate predictions, so it is chosen in this study.

Table 1. New LUTs of Chinese Medicinal Yam added in AEZ model

NAME	CYA+CYB	TMN	TREF	HI	MLAI	YF%	TS2n	TS1n	TS1x	TS2x
YAM M1	0 + 180	10.0	23.0	0.50	3.00	0.51	3400	3750	4250	4500
YAM M2	0 + 195	10.0	22.5	0.50	3.00	0.54	3600	4000	4500	4750

YAM M3	0 + 210	10.0	22.0	0.50	3.00	0.57	4000	4400	4850	5200

LUTs: Land utilization types; TS2: the lower and upper boundaries of accumulated heat units range; TS1: optimum accumulated heat units; TS3: the accumulated temperature above 10 degrees; HI: the harvest index; MLAI: Maximum Leaf Area Index;

3 Results

3.1 Climate simulation and the climate change in semi-arid regions

As this study focuses on the semi-arid regions, the CMY genuine production area in North China is selected as the study area, which includes parts of semi-wet regions. Figure 1 shows the topography of the study area and the red provinces are genuine CMY production areas. As the CMY planting and growing period are mainly from May to October, the daily average temperature, daily maximum temperature and daily mini-mum temperature in that period are shown in Figure 2. For most parts of the study area, PRECIS overestimates the daily mean temperature by 1–3^{o}C, while HadGEM2-ES underestimates a little in the southern part. PRECIS is more consistent with the observations in the northeastern part. For daily maximum temperature, the simulations show similar spatial pattern with the daily mean temperature, with a warm bias (less than 2^{o}C) in most areas, which is contrast to the cold bias by HadGEM2-ES in the southern part. A clear improvement is shown in Figure 1i that PRECIS represents daily minimum temperature more accurate than HadGEM2-ES, with the bias ranging from −1 to 1^{o}C in most parts.

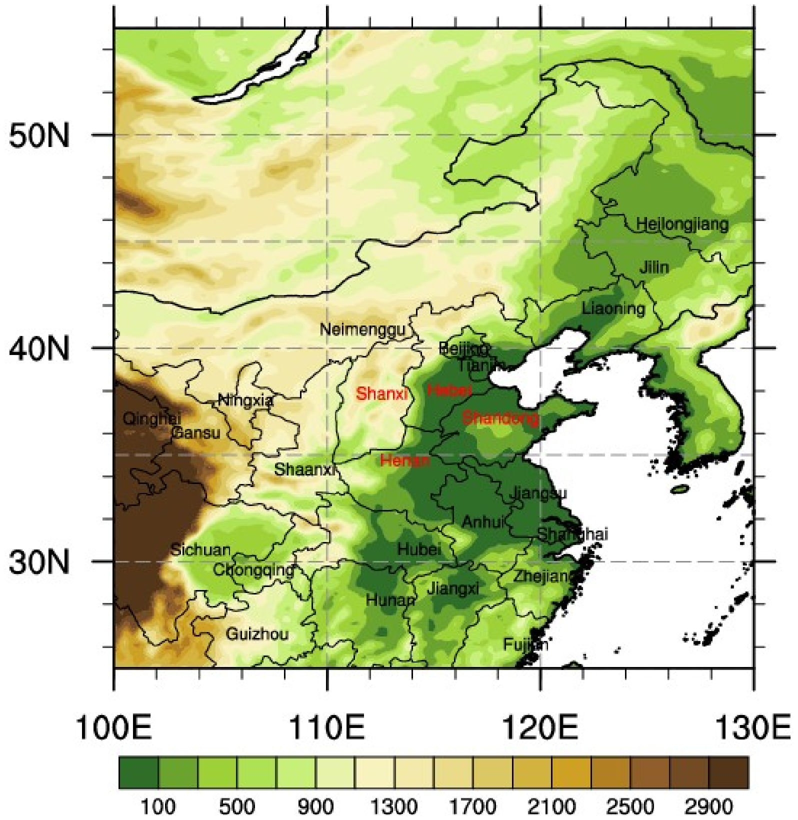

Figure 1. Study domain and the topography within it (unit: m). The red provinces are main producing area of CMY.

Besides temperature, precipitation also plays an essential role in agrometeorology. Figure 3 shows the annual and growing-period average precipitation observed during 1986–2005 and the deviations between model simulations and the observations. In the simulations, the annual and growing-period average precipitation is underestimated in the southeast while overestimated in the northwest. The bias in the growing period is smaller than that in the whole year. The bias of HadGEM2-ES is transmitted to PRECIS to a certain extent, as the bias spatial distribution and value of PRECIS correspond well with the HadGEM2-ES. PRECIS underestimates the annual precipitation in Shandong, Henan and their surrounding areas. The underestimation is also found in the growing period, while the overestimation in the northern part is much smaller.

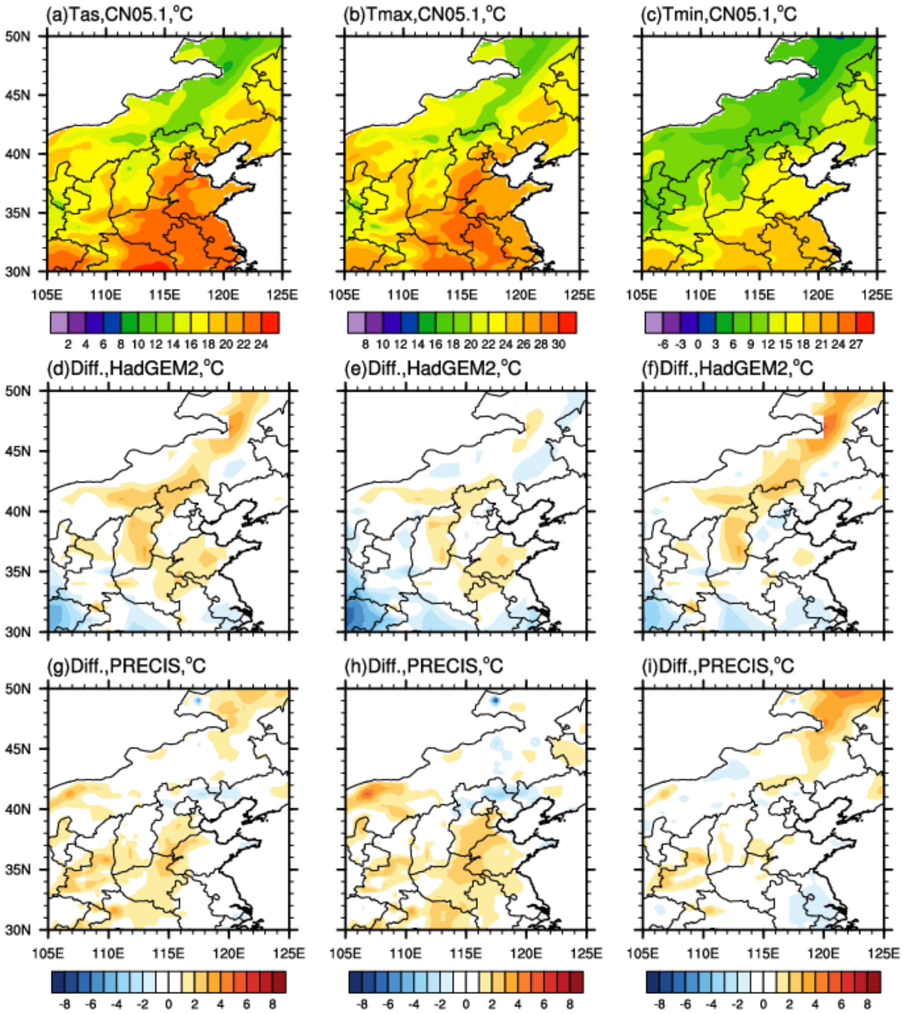

Figure 2. Observed (a) daily mean, (b) maximum and (c) minimum temperatures in CMY growing period (GP, May–October), and the model biases with the observations ((d) and (g) correspond with (a); (e) and (h) correspond with (b); (f) and (i) correspond with (c)).

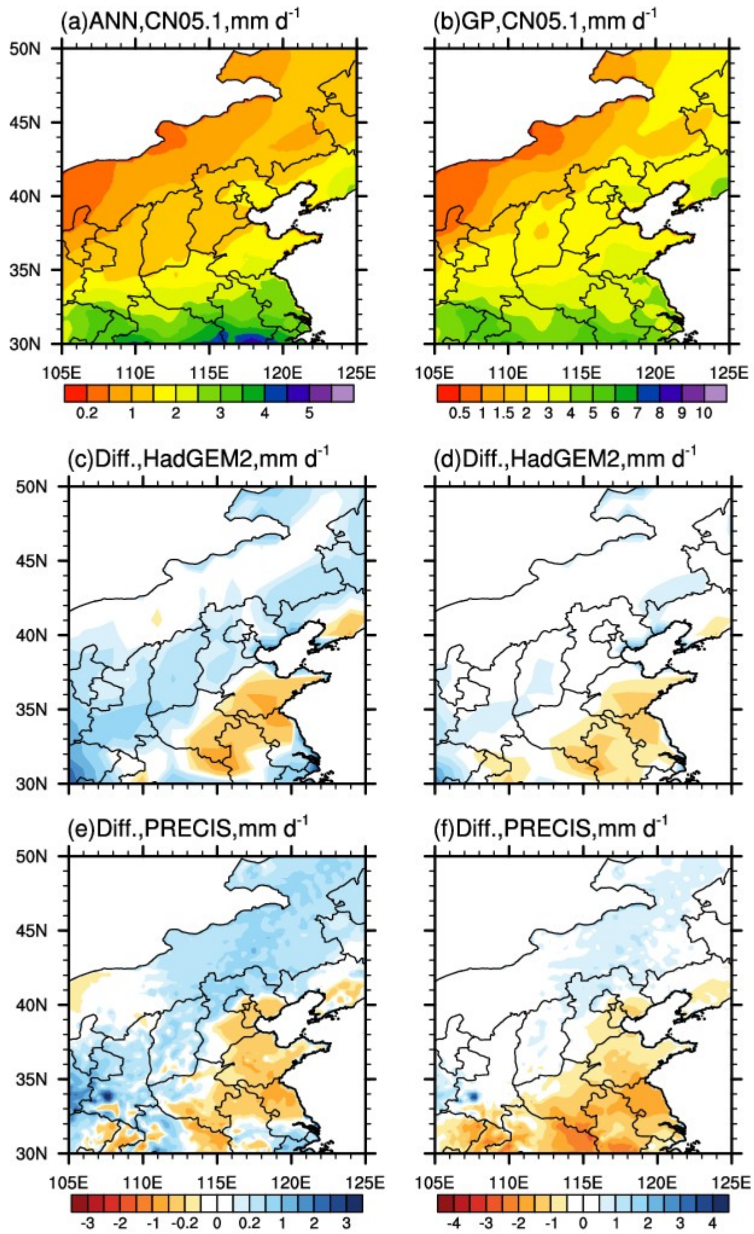

Figure 3. Observed daily mean precipitation in (a) ANN (annual) and (b) GP, and the model biases with the observations (c) and (e) correspond with (a); (d) and (f) correspond with (b)).

Though the improvement of PRECIS in average temperature or precipitation is not so obvious as HadGEM2-ES in the study area, the benefits are recognized in other regions or extreme indexes (Jiang et al., 2020; Dong et al., 2020). Moreover, the temperature bias shown in Figure 2g,i at Hebei and Shandong is smaller by PRECIS, where is genuine CMY production region. The CMY simulation is mainly under irrigation condition in this article, so the precipitation bias is not so important while PRECIS remains well reality. As shown in Figure 4, under the RCP8.5 scenario during 2031–2050, the temperature in the study area will be 1.5 ºC higher than that in 1986–2005, and the maximum daily temperature may increase by 3 ºC in local regions. The average temperature simulated by PRECIS increases more in the areas near Henan than that by HadGEM2-ES. Such spatial pattern difference of temperature may come from a better representation of topography. The temperature variation differs between the provincial boundaries of Shanxi and Hebei, where locates the Taihang Mountains. The seasonal variations of daily maximum temperature and daily minimum temperature are similar to that of the daily average temperature to a certain extent (figure omitted).

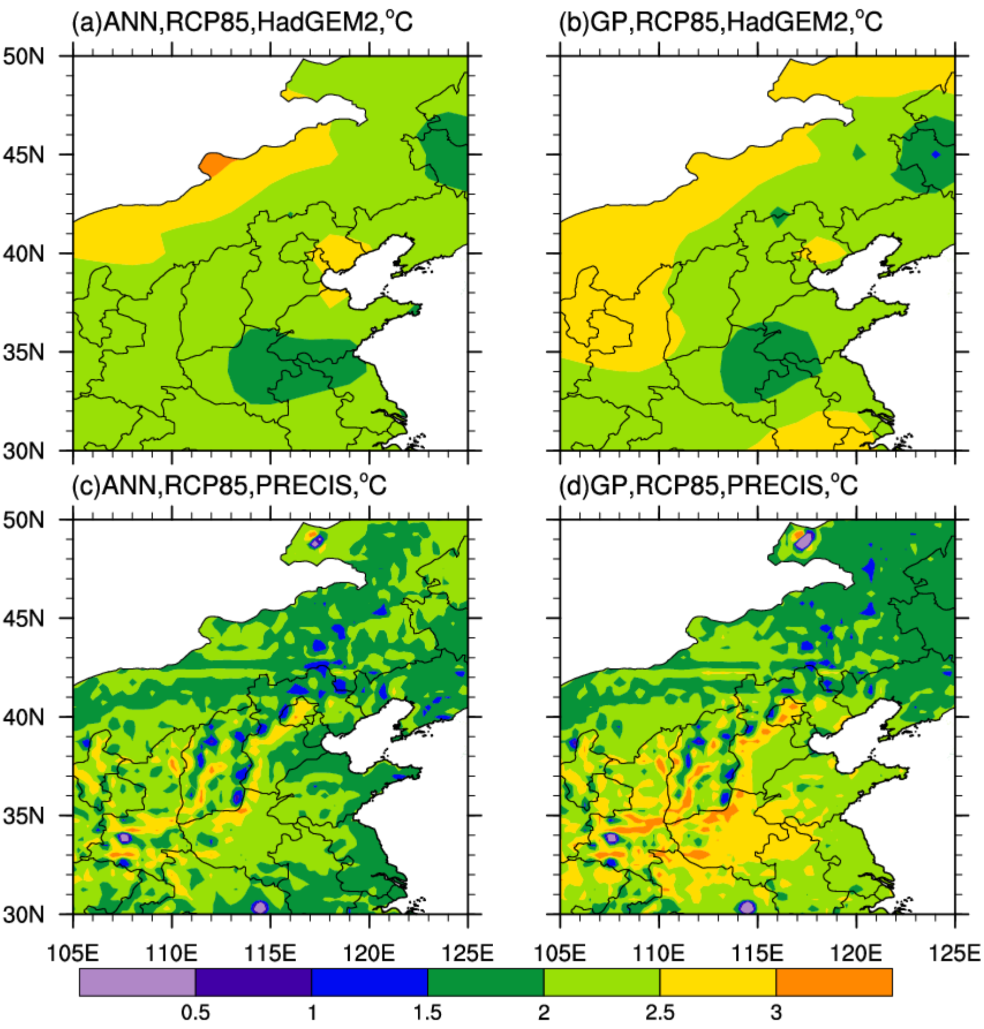

Figure 4. The spatial patterns of the daily mean temperature change in (a, c) the whole year and (b, d) the growing-period (unit: ^{o}C).

Figure 5 shows the change of average precipitation in the future during 2031–2050 relative to 1986–2005. The annual precipitation will increase in almost all regions, with the maximum increase of more than 30% in PRECIS. There is little difference between the HadGEM2-ES projection and the historical period. The change range of annual precipitation in each region is relatively uniform, concentrated within 20%. PRECIS and HadGEM2-ES have good consistency in the annual precipitation, but PRECIS projects a precipitation decrease in more regions, especially in the northeast. The changes in GP fluctuate more than that in the annual average. In many parts of CMY genuine producing area, PRECIS also projects less precipitation in GP, such as in the northern Henan, western Shanxi and northern Hebei, and the decrease can reach 20% locally.

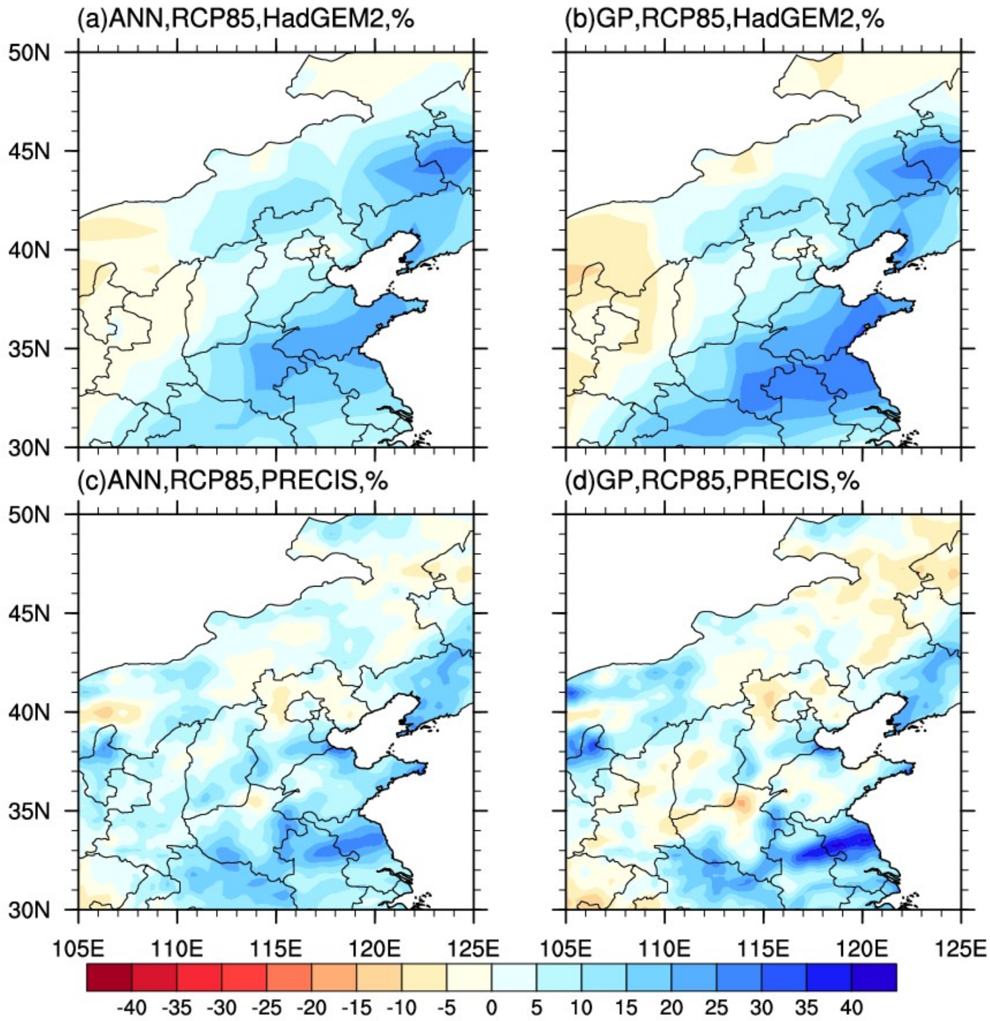

Figure 5. The spatial patterns of the future precipitation change in (a, c) the whole year and (b, d) the growing-period (unit: %).

Global warming will bring further increase of heat resources in most areas, which has been a consistent recognition. Accumulated temperature refers to the sum of daily average temperature in the growing stage of crops. The accumulated temperature above 10 ^{o}C is an important index to measure agricultural climate heat resources, because CMY is thermophilic crops. By the 2050s, under the both scenario, the accumulated temperature (above 10 ^{o}C) will generally increase in the growing season in China, and most of the temperature increase in genuine producing areas is above 450 ^{o}C under RCP4.5 and above 800oC under RCP8.5 (Figure 6). Under the influence of climate warming, the heat resources that can satisfy the growth and development of crops are further enriched, so the accumulated temperature increases significantly. Therefore, the heat resources are more abundant, which is the consistent impact of global warming on agricultural cli-mate resources.

The length of the growing season in agroclimatic resources is an important index to comprehensively consider the heat, moisture, radiation and other regional resources. It represents the length of the period suitable for agricultural planting in a region in a year, which is of great significance to deploying crop sowing time and planting systems. The growing season in the AEZ model is defined as the number of days that the crop actual evapotranspiration (ETA) is greater than or equal to 50 percent of the reference evapotranspiration (ET0) above the critical temperature of 5 ^{o}C. Under the future climate scenario, the change of meteorological factors, such as temperature, precipitation and evapotranspiration, will result to a general extension of the growing season (Figure 7). The growing season in the northern region, where the original growing season is short, may also have a general extension . Due to the warmer and wetter climate conditions, the growing season in the genuine yam area is extended by more than 20 days.

Evapotranspiration plays an important role in the earth's atmosphere-hydrosphere-biosphere. Together with precipitation, it could determine the regional dry and wet conditions, and plays a key role in estimating ecological water de-mand and agricultural irrigation. In the AEZ model, the Penman-Monteith formula recommended by UN-FAO is used to calculate the reference crop evapotranspiration. Assuming that the reference crop height is 0.12 m, the crop canopy resistance is a constant of 70 m s^{-1} and the surface reflectance is 0.23, then the reference crop evapotranspiration could be calculated. Under the baseline climate condition, the evapotranspiration of yam road is more than 500 mm A^{-1} (not shown). The evapotranspiration in the east and the south will increase in the future. The increase of evapotranspiration in the yam production area is mostly within 60 mm A^{-1} under the RCP4.5 scenario, and more under the RCP8.5 scenario (Figure 8).

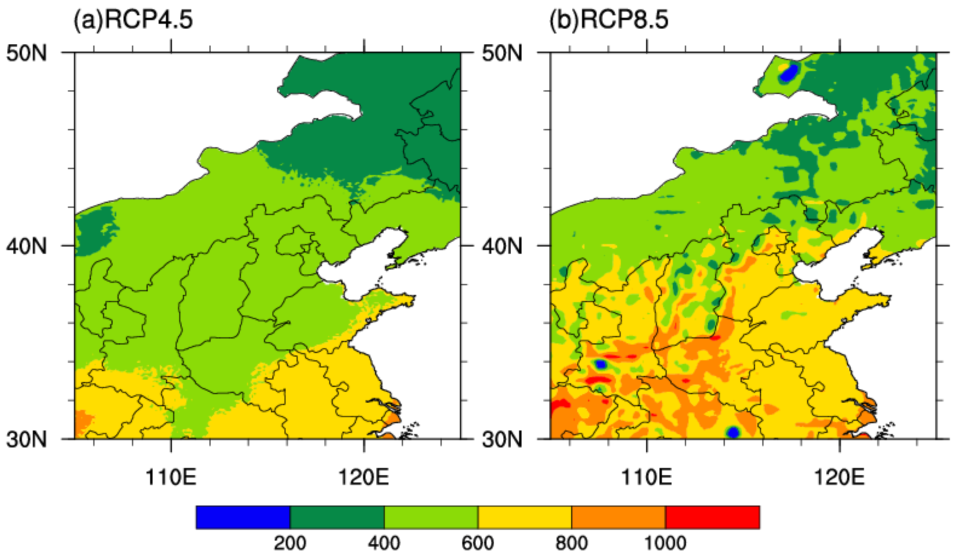

Figure 6. The change of accumulated temperature (above 10ºC) in the 2050s com-pared with the baseline for (left) the RCP4.5 and (right) RCP8.5 scenarios.

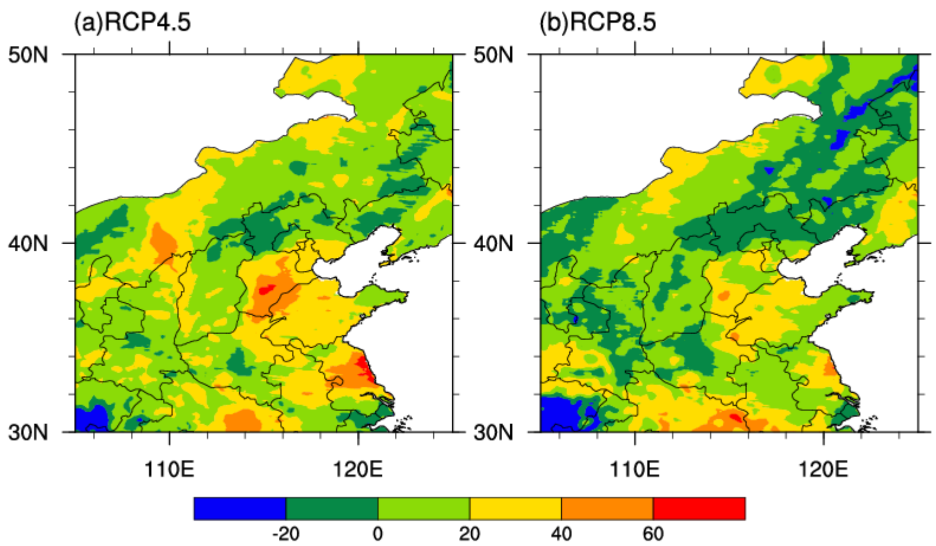

Figure 7. The change of growing period length in the 2050s compared with the baseline for (left) the RCP4.5 and (right) RCP8.5 scenarios.

.

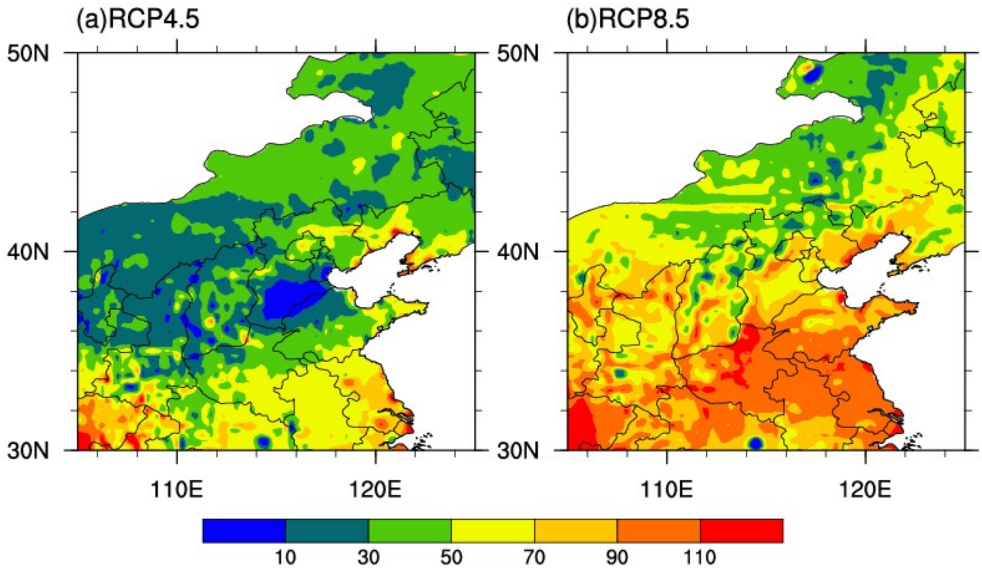

Figure 8. The change of reference evapotranspiration in the 2050s compared with the baseline for (left) the RCP4.5 and (right) RCP8.5 scenarios.

3.2 Simulating the CMY yield under future climate scenarios

Under the historical climate conditions, the suitable regionalization of CMY is shown in Figure 9. It can be seen that the simulated dry weight yield of CMY is more than 3000 kg ha^{-1}, that is, 200 kg mu^{-1}. Because of the high drying rate of yam, the water accounts for about 70% and the dry matter is about 30%. Suppose the dry weight is 200–500 kg mu^{-1}, and then it could be converted into the fresh weight, which is about 700–1700 kg mu^{-1}, very close to the current unit yield (1000–1500 kg mu^{-1}) in the main production areas of CMY. The AEZ model output are in the same range of the observed yield values of the typical CMY production area. The PRECIS simulation also well meets this feature. The maximum yield of PRECIS simulation is slightly larger than that of another observation data set (CRUTS32). It may be related to the fact that the model summer is warmer than observations in the growth suitable areas, because the quality of heat conditions will affect the growth and development of crops and determine the formation speed of yam organs, thus affecting its yield.

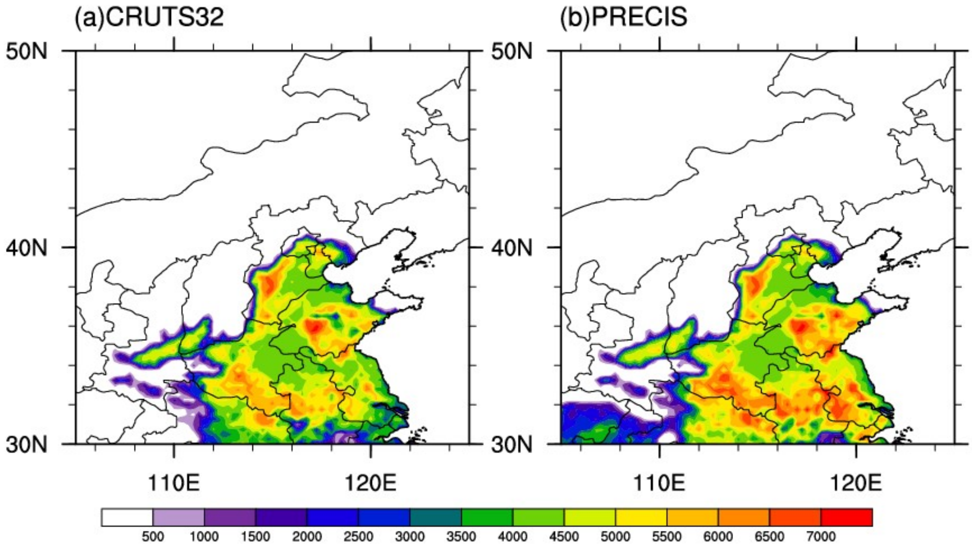

Figure 9. The CMY yield (kg DM mu^{-1}) in the suitable planting areas under the historical climate (Left: CRUTS32, 8110; right: PRECIS, 1986–2005).

By comparing and analyzing the suitability zoning of CMY under the historical climate conditions and the climate scenarios in the middle of this century, the suitable planting areas under future climate scenarios are superimposed with the suitable areas under the historical climate conditions. The results are shown in the Figure 10. The PRECIS predicts that the suitable areas of CMY in Shandong, Henan and Hebei provinces would remain suitable during the 2050s. The suitable areas of Shaanxi, Shanxi and Shandong are significantly expanded, and the suitable areas also appear in Liaoning Province. Considering the suitable areas, there are no significant differences between the RCP8.5 and RCP4.5 scenarios. But there is a larger suitable area in the northeast under the RCP8.5 scenario.

The northward extension of the suitable area is mainly due to the enrichment of heat resources and water-soil conditions under the influence of climate warming. In addition to the extreme precipitation risk, the impact of precipitation change on the CMY growth is relatively small because it mainly relies on irrigation, and the impact of extreme precipitation on yam yield needs further studies.

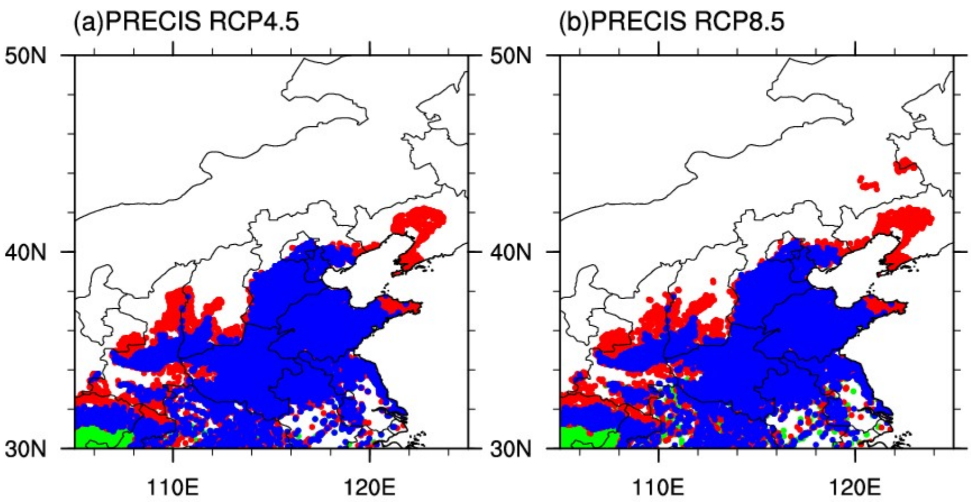

Figure 10. The change of the suitable area for CMY in 2050s comparing with the baseline for (a) the RCP4.5 scenario and (b) the RCP8.5 scenario in PRECIS. red : unsuitable -> suitable, green: suitable -> unsuitable, blue: suitable -> suitable

The PRECIS simulations show there will be a small reduction in CMY production in the existing areas, while the unit yield in Shaanxi and Shanxi will increase slightly, but most of the increased production will be distributed in the newly added yam production areas (Figure 11, Table 2,3). In Shandong and Liaoning, the output in new production areas is larger, but less than the historical maximum level. In addition, the growth in the northernmost part of the study region is not much, which indicates that only the suit-ability of yam planting appears in this region, but the yield could not be guaranteed. According to the map (Figure 6,8), the increase of accumulated temperature may in-crease evaporation and cause water waste. At the same time, it will also shorten the growth period of crops, which will affect the accumulation of nutrients and reduce the yield in Henan Province and other regions.

Hu (2019) projected that the unit output in eastern Shandong and eastern Hebei will increase in 2050, while in some western regions it will decrease. The unit yield in the eastern part of Henan Province will decrease, while that in the western region will in-crease. In most areas of central and southern Shanxi, the unit yield will decrease. Overall, in Hu (2019) the yield in the traditional production area decreases, but there are some new production areas in the northeast. His conclusions are consistent with the simulation results in our study.

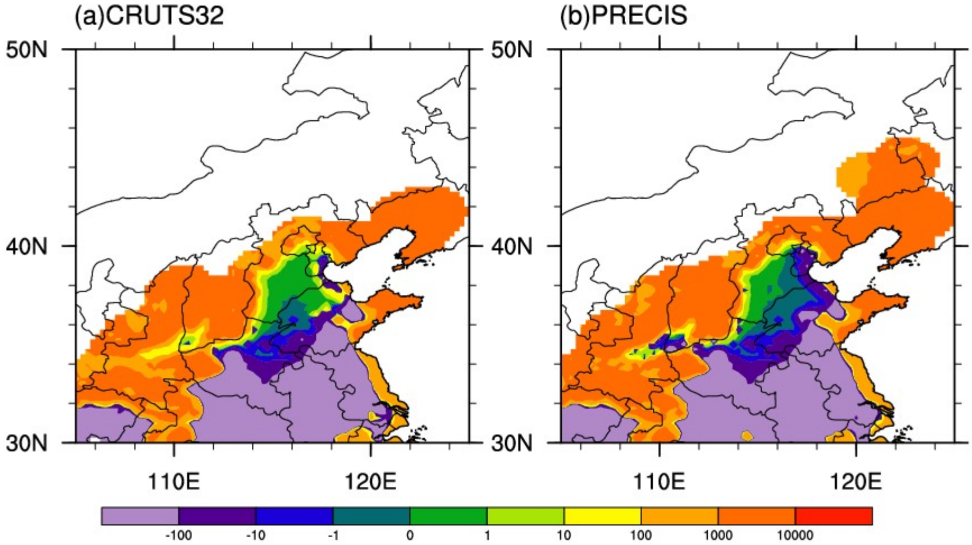

Figure 11. The change of the CMY yield (kg DM) in the 2050s under (a) the RCP4.5 scenario and (b) RCP8.5 scenario in PRECIS.

Table 2. Output changes of CMY under RCP4.5

	Decrease area(km^2)	**Increase area(km^2)**	**Cumulative change(t)**
Shanxi	166	16470	33468
Shandong	24610	26777	55437
Henan	54991	5706	-12820
Hebei	418	8597	17427
Liaoning	-	16490	65926
Gansu	-	3998	4912
Shaanxi	696	32129	57022
Total	80881	110167	221372

Table 3. Output changes of CMY under RCP8.5

	Decrease area(km^2)	Increase area(km^2)	Cumulative change(t)
Shanxi	944	10195	24088
Shandong	16228	21158	43894
Henan	43035	2406	-12675
Hebei	864	4051	11525
Liaoning	-	13054	56410
Gansu	-	3153	6375
Shaanxi	1861	12935	24365
Total	62942	66952	153982

4 Conclusion and Discussion

Future climate conditions remain considerable uncertainties, though existing studies have made many climate projections over China (Xu et al., 2019; He et al., 2019). There is a shortage of literature assessing the impacts of climate change on agroclimatic conditions based on high-resolution RCMs (Tian et al., 2014; Tian et al., 2015). This study focuses on the agroclimatic change based on a high-resolution RCM in China, providing an overall impression of agriculture yield over semi-arid regions, and then projects the yield and the suitable area for the CMY in the 2050s.

To verify the simulation ability of PRECIS in semi-arid regions and find its advantages compared to the GCMs, the historical simulation is evaluated first. Though PRECIS simulation does not show the significant advantage in precipitation amount, the PRECIS simulation of average temperature is more in line with the observations in most parts of the country, which is significantly better than the simulation of HadGEM2-ES. In 2031–2050, under the RCP8.5 scenario, the temperature in most parts of China will generally rise by more than 1.5ºC in PRECIS. The high-temperature days will increase, and the low-temperature days will decrease. For the average annual precipitation, there will be about 10% more in the future nationwide, but there is a possibility of a decrease in North China. The precipitation increase is larger in the growing period, reaching 20% by HadGEM2-ES, while PRECIS projects a decrease in local regions of genuine production areas.

Under the influence of climate warming, the heat resources that can satisfy the growth and development of crops are further enriched, so the accumulated temperature increases significantly. The accumulated temperature increases by about 500^{o}C in the CMY genuine areas over the semi-arid regions. The length of the growing season in the genuine yam area will extend slightly, while will decrease in other arid and semi-arid regions. The evapotranspiration in the northwest or north China may slightly increase by no more than 80 mm.

Because the temperature conditions in the north could meet the growth needs of yam due to the climate warming in the future, the CMY production areas will expand northward, and more than 10,000 km^2 new suitable areas will appear in Liaoning. The traditional yam production areas are still suitable for yam production. The CMY yield will increase, which is the result of the increased suitable plating areas and unit area yield.

The future climate change has been reported to influence the botany spatial distribution and their local ecosystems. Zhang et al. (2018) reported a continuous rising-temperature might decrease the suitable habitat of Paeonia delavayi which lives in the southwest mountain region of China. Climate change also might affect the G. rigescens in the southwest of China, making habitat moving to higher elevation (Shen et al., 2021). More than 1000 woody plant suffer from loss of distribution areas in Yunnan due to extreme climate change (Zhang et al., 2014).

This study uses a high-resolution RCM to simulate the future CMY yield. However, there must be large uncertainties and systematic deviations in a single model. In future studies, there is still some improving room by using higher-resolution RCMs. Moreover, climate condition is not the only impact of crop growth, so further researches are needed to better understand which factors could determine the CMY quality of the medicinal components (Fan et al., 2019).

Acknowledgement: This research was funded by THE NATIONAL KEY R&D PROGRAM OF CHINA, grant number 2019YFE0124800, THE NATIONAL NATURAL SCIENCE FOUNDATION OF CHINA, grant number 51761135024 and THE HIGH-LEVEL SPECILA FUNDING OF THE SOUTHERN UNI-VERSITY OF SCIENCE AND TECHNOLOGY, grant number G02296302 and G02296402. The dataset is available at https://osf.io/74caq/ .

References

1. Bellouin, N., Collins, W. J., Culverwell, I. D., Halloran, P. R., Hardiman, S. C., Hinton, T. J., ... & Wiltshire, A. (2011). The HadGEM2 family of met office unified model climate configurations. *Geoscientific Model Development, 4*(3), 723-757.
2. Bucchignani, E., Zollo, A. L., Cattaneo, L., Montesarchio, M., and Mercogliano, P. (2017). Extreme weather events over China: assessment of COSMO‐CLM simulations and future scenarios. *International Journal of Climatology, 37*, 1578-1594.
3. Bouras, E., Jarlan, L., Khabba, S., Er-Raki, S., Dezetter, A., Sghir, F., & Tramblay, Y. (2019). Assessing the impact of global climate changes on irrigated wheat yields and water requirements in a semi-arid environment of Morocco. *Scientific reports , 9*, 1-14.
4. Chen, N., and Gao, X. Climate change in the twenty-first century over China: projections by an RCM and the driving GCM. (2019). *Atmospheric and Oceanic Science Letters, 12*, 270-277. doi:10.1080/16742834.2019.1612695
5. Duan, W., Hanasaki N., Shiogama H., Chen Y., Zou S., Nover D., Zhou B., and Wang Y. (2019). Evaluation and Future Projection of Chinese Precipitation Extremes Using Large Ensemble High-Resolution Climate Simulations. *Journal of Climate, 32*, 2169-2183. doi:10.1175/jcli-d-18-0465.1
6. Dong, G., Jiang, Z., Tian, Z., Buonomo, E., Sun, L., and Fan, D. (2020). Projecting Changes in Mean and Extreme Precipitation over Eastern China during 2041–2060. *Earth and Space Science, 7*, e2019EA001024. https://doi.org/10.1029/2019EA001024
7. Du, J., He, Z., Piatek, K. B., Chen, L., Lin, P., & Zhu, X. (2019). Interacting effects of temperature and precipitation on climatic sensitivity of spring vegetation green-up in arid mountains of China. *Agricultural and Forest Meteorology, 269*, 71-77.
8. Fan, D., Zhong, H., Hu, B., Tian, Z., Sun, L., Fischer, G., Wang, X., Jiang, Z. (2019) Agro-ecological suitability assessment of Chinese Medicinal Yam under future climate change. *Environmental Geochemistry and Health*, 1-14.
9. Fernández, F. J., Blanco, M., Ponce, R. D., Vásquez-Lavín, F., & Roco, L. (2019). Implications of climate change for semi-arid dualistic agriculture: a case study in Central Chile. *Regional Environmental Change, 19*, 89-100.
10. Fischer, G., Shah, M., N. Tubiello, F., & Van Velhuizen, H. (2005). Socio-economic and climate change impacts on agriculture: an integrated assessment, 1990–2080. *Philosophical Transactions of the Royal Society B: Biological Sciences, 360*, 2067-2083.
11. Fischer, G., Van Velthuizen, H., Nachtergaele, F., Medow, S. (2000). Global

Agro-Ecological Zones (Global -AEZ) CD-ROM FAO/IIASA.
12. Fischer, G., Van Velthuizen, H. T., Shah, M. M., & Nachtergaele, F. O. (2002). Global Agro-Ecological Assessment for Agriculture in the 21st Century: Methodology and Results. IIASA: Laxenburg, Austria
13. Giorgi, F., Jones, C., and Asrar, G. R. (2009). Addressing climate information needs at the regional level: the CORDEX framework. *World Meteorological Organization (WMO) Bulletin, 58*, 175-183.
14. Gu, H., Yu, Z., Yang, C., Ju, Q., Yang, T., and Zhang, D. (2018). High-resolution ensemble projections and uncertainty assessment of regional climate change over China in CORDEX East Asia. *Hydrology and Earth System Sciences, 22*, 3087.
15. Guo, J., Huang, G., Wang, X., & Li, Y. (2019). Improved performance of a PRECIS ensemble in simulating near-surface air temperature over China. *Climate dynamics, 52*, 6691-6704.
16. Han, Z., Shi, Y., Wu, J., Xu, Y., and Zhou, B. (2019). Combined dynamical and statistical downscaling for high-resolution projections of multiple climate variables in the Beijing–Tianjin–Hebei region of China. *Journal of Applied Meteorology and Climatology, 58*, 2387-2403.
17. He, W.-p., Zhao, S.-s., Wu, Q., & Wan, S. (2019). Simulating evaluation and projection of the climate zones over China by CMIP5 models. *Climate Dynamics, 52*, 2597-2612.
18. Harris, I. P. D. J., Jones, P. D., Osborn, T. J., & Lister, D. H. (2014). Updated high−resolution grids of monthly climatic observations–the CRUTS3.10 Dataset. *International journal of climatology, 34*(3), 623-642.
19. Hu, B. (2019). Agro-Ecological Suitability Analysis of Chinese Medicinal Yam under Future Climate Change. Master Thesis, Shanghai Institute of Technology, Shanghai, China.
20. Hu, B., Fan, D., Tian, Z., Xu, H., Ji, Y., & Wang, X. (2018). Analysis on ecological suitability planting area of Chinese medicinal yam. In 2018 7th International Conference on Agro-geoinformatics (Agro-geoinformatics) August 2018; pp. 1-4. IEEE.
21. Huang, J., Ma, J., Guan, X., Li, Y., & He, Y. (2019). Progress in semi-arid climate change studies in China. *Advances in Atmospheric Sciences, 36*, 922-937.
22. Hui, P., Tang, J., Wang, S., Niu, X., Zong, P., and Dong, X. (2018). Climate change projections over China using regional climate models forced by two CMIP5 global models. Part I: evaluation of historical simulations. *International Journal of Climatology, 38*, e57-e77.
23. IPCC. (2018). Special Report on Global Warming of 1.5 °C.
24. Jiang, Z., Tian, Z., Dong, G., Sun, L., Zhang, P., Erasmo, B., Fan, D. (2020). High-resolution projections of mean and extreme precipitation over China by two regional climate models. *J. Meteor. Res, 34*, 1–22, doi: 10.1007/s13351-020-9208-5
25. Kong, X., Wang, A., Bi, X., and Wang, D. (2019). Assessment of Temperature

Extremes in China Using RegCM4 and WRF. *Advances in Atmospheric Sciences ,* *36*, 363-377.
26. Kourat, T., Smadhi, D., Mouhouche, B., Gourari, N., Amin, M. M., & Bryant, C. R. (2020). Assessment of future climate change impact on rainfed wheat yield in the semi-arid Eastern High Plain of Algeria using a crop model. *Natural Hazards*, 1-29.
27. Kukal, M. S., & Irmak, S. (2018). Climate-driven crop yield and yield variability and climate change impacts on the US Great Plains agricultural production. *Scientific Reports, 8*, 1-18.
28. Li, Y., Huang, J., Ji, M., & Ran, J. (2015). Dryland expansion in northern China from 1948 to 2008. *Advances in Atmospheric Sciences, 32*, 870-876.
29. Mo, X. G., Hu, S., Lin, Z. H., Liu, S. X., & Xia, J. (2017). Impacts of climate change on agricultural water resources and adaptation on the North China Plain. *Advances in Climate Change Research, 8*, 93-98.
30. Moonen, A. C., Ercoli, L., Mariotti, M., & Masoni, A. (2002). Climate change in Italy indicated by agrometeorological indices over 122 years. *Agricultural and Forest Meteorology, 111*, 13-27.
31. Niu, X., Wang, S., Tang, J., Lee, D.−K., Gutowski, W., Dairaku, K., McGregor, J., Katzfey, J., Gao, X., Wu, J., Hong, S.−y., Wang, Y., Sasaki, H. and Fu, C. (2018). Ensemble evaluation and projection of climate extremes in China using RMIP models. *International Journal of Climatology, 38*, 2039-2055. doi:10.1002/joc.5315
32. Park, C., and Min, S. (2019). Multi-RCM near-term projections of summer climate extremes over East Asia. *Climate Dynamics, 52*, 4937-4952.
33. Parry, M. L. (2019). Climate change and world agriculture. Routledge.
34. Sun, Q., Miao, C., and Duan, Q. (2015). Comparative analysis of CMIP3 and CMIP5 global climate models for simulating the daily mean, maximum, and minimum temperatures and daily precipitation over China. *Journal of Geophysical Research: Atmospheres, 120*, 4806-4824. doi:10.1002/2014jd022994
35. Shen, T., Yu, H., & Wang, Y. Z. (2021). Assessing the impacts of climate change and habitat suitability on the distribution and quality of medicinal plant using multiple information integration: Take Gentiana rigescens as an example. *Ecological Indicators, 123*, 107376.
36. Shkolnik, I. M., Pigol'tsina, G. B., & Efimov, S. V. (2019). Agriculture in the Arid Regions of Eurasia and Global Warming: RCM Ensemble Projections for the Middle of the 21st Century. *Russian Meteorology and Hydrology, 44*, 540-547.
37. Singh, N., Mall, R. K., Sonkar, G., Singh, K. K., & Gupta, A. (2018). Evaluation of RegCM4 climate model for assessment of climate change impact on crop production. *Evaluation, 551*, 631-55.
38. Tian, Z., Liang, Z., Sun, L., Zhong, H., Qiu, H., Fischer, G., & Zhao, S. (2015). Agriculture under climate change in China: Mitigate the risks by grasping the

emerging opportunities. *Human and Ecological Risk Assessment: An International Journal, 21*, 1259-1276.
39. Tian, Z., Yang, X., Sun, L., Fischer, G., Liang, Z., & Pan, J. (2014). Agroclimatic conditions in China under climate change scenarios projected from regional climate models. *International journal of climatology, 34*, 2988-3000.
40. Tian, Z., Zhong, H., Shi, R., Sun, L., Fischer, G., & Liang, Z. (2012). Estimating potential yield of wheat production in China based on cross-scale data-model fusion. *Frontiers of Earth Science, 6*, 364-372.
41. Wu, Y., Guo, J., Lin, H., Bai, J., & Wang, X. (2020). Spatiotemporal patterns of future temperature and precipitation over China projected by PRECIS under RCPs. *Atmospheric Research, 249*, 105303.
42. Wu, J., Gao X. (2013). A gridded daily observation dataset over China region and comparison with the other datasets. *Chinese J. Geophys, 56*(4), 1102-1111, (in Chinese). doi: 10.6038/cjg20130406.
43. Wang, R., Cheng, Q., Liu, L., Yan, C., & Huang, G. (2019). Multi-model projections of climate change in different RCP scenarios in an arid inland region, Northwest China. *Water, 11*, 347.
44. Waldman, K. B., Attari, S. Z., Gower, D. B., Giroux, S. A., Caylor, K. K., & Evans, T. P. (2019). The salience of climate change in farmer decision-making within smallholder semi-arid agroecosystems. *Climatic Change, 156*, 527-543.
45. Xia, J., Ning, L., Wang, Q., Chen, J., Wan, L., & Hong, S. (2017). Vulnerability of and risk to water resources in arid and semi-arid regions of West China under a scenario of climate change. *Climatic Change, 144*, 549-563.
46. Xu, K., Xu, B., Ju, J., Wu, C., Dai, H., and Hu, B. X. (2019). Projection and uncertainty of precipitation extremes in the CMIP5 multimodel ensembles over nine major basins in China. *Atmospheric Research, 226*, 122-137. doi:10.1016/j.atmosres.2019.04.018
47. Xu, Z., & Yang, Z. L. (2017). Relative impacts of increased greenhouse gas concentrations and land cover change on the surface climate in arid and semi-arid regions of China. *Climatic Change, 144*, 491-503.
48. Yang, Y., Bai, L., Wang, B., Wu, J., & Fu, S. (2019). Reliability of the global climate models during 1961–1999 in arid and semiarid regions of China. *Science of the Total Environment, 667*, 271-286.
49. Zhang, D., Han, Z., and Shi, Y. (2017). Comparison of climate projections between driving CSIRO-Mk3.6.0 and downscaling simulation of RegCM4.4 over China. *Advances in Climate Change Research, 8*, 245-255. doi:10.1016/j.accre.2017.10.001
50. Zhang, K., Yao, L., Meng, J., & Tao, J. (2018). Maxent modeling for predicting the potential geographical distribution of two peony species under climate change. *Science of the Total Environment, 634*, 1326-1334.
51. Zhang, M. G., Zhou, Z. K., Chen, W. Y., Cannon, C. H., Raes, N., & Slik, J. F. (2014). Major declines of woody plant species ranges under climate change in Y

unnan, C hina. *Diversity and Distributions, 20*, 405-415.

52. Zou, J., Xie, Z., Zhan, C., Chen, F., Qin, P., Hu, T., & Xie, J. (2019). Coupling of a Regional Climate Model with a Crop Development Model and Evaluation of the Coupled Model across China. *Advances in Atmospheric Sciences, 36*, 527-540.